Identifying intrinsic and reflexive contributions to low-back stabilization

van Drunen, P.; Maaswinkel, E.; van der Helm, F.C.T.; van Dieen, J.H.; Happee, R.

published in
Journal of Biomechanics
2013

DOI (link to publisher)
10.1016/j.jbiomech.2013.03.007

Journal of Biomechanics 46 (2013) 1440–1446

Contents lists available at SciVerse ScienceDirect

Journal of Biomechanics

journal homepage: www.elsevier.com/locate/jbiomech
www.JBiomech.com

Identifying intrinsic and reflexive contributions to low-back stabilization

P. van Drunen [a,*], E. Maaswinkel [b], F.C.T. van der Helm [a], J.H. van Dieën [b], R. Happee [a]

[a] BioMechanical Engineering Department, Faculty of Mechanical Engineering, Delft University of Technology, Mekelweg 4, 2628 CD Delft, The Netherlands
[b] MOVE Research Institute Amsterdam, Faculty of Human Movement Sciences, VU University Amsterdam, van der Boechorststraat 9, 1081 BT Amsterdam, The Netherlands

ARTICLE INFO

Article history:
Accepted 5 March 2013

Keywords:
Lumbar Spine
Postural control
System identification
Muscle spindles
Golgi tendon organ

ABSTRACT

Motor control deficits have been suggested as potential cause and/or effect of a-specific chronic low-back pain and its recurrent behavior. Therefore, the goal of this study is to identify motor control in low-back stabilization by simultaneously quantifying the intrinsic and reflexive contributions. Upper body sway was evoked using continuous force perturbations at the trunk, while subjects performed a resist or relax task. Frequency response functions (FRFs) and coherences of the admittance (kinematics) and reflexes (sEMG) were obtained. In comparison with the relax task, the resist task resulted in a 61% decrease in admittance and a 73% increase in reflex gain below 1.1 Hz. Intrinsic and reflexive contributions were captured by a physiologically-based, neuromuscular model, including proprioceptive feedback from muscle spindles (position and velocity) and Golgi tendon organs (force). This model described on average 90% of the variance in kinematics and 39% of the variance in sEMG, while resulting parameter values were consistent over subjects.

1. Introduction

Low-back pain (LBP) is a common disorder, which affects 40–60% of the adult population annually in Western Europe and North America (Loney and Stratford, 1999; Picavet and Schouten, 2003). The effect of most treatments (e.g., anti-inflammatory drugs, neuromuscular training and cognitive therapy) is fairly small, and 60–75% of the patients have recurrent symptoms within a year with 10% developing chronic LBP (van den Hoogen et al., 1998). Motor control deficits (e.g., delayed 'reflex' responses, increased antagonistic co-contraction) have been suggested as potential cause and/or effect of LBP and its recurrent behavior (Cholewicki et al., 2000; Radebold et al., 2001; van Dieën et al., 2003).

Motor control provides an essential contribution to low-back stabilization, since the spine is inherently unstable without active musculature in spite of stiffness and damping provided by passive tissue (Bergmark, 1989; Crisco and Panjabi, 1991). The muscular contribution to stabilization of the spine involves muscle viscoelasticity and reflexive feedback. Muscle viscoelasticity comprises the stiffness and damping of the muscles and can be altered by co-contraction and selective muscle activity. Given the limited contribution of passive tissues especially in upright trunk postures and the difficulty to separate these components, properties of passive tissues and muscle viscoelasticity are usually lumped into intrinsic stiffness and damping. Feedback comprises visual, vestibular and proprioceptive contributions, where the latter is based on information of muscle length and muscle lengthening velocity from muscle spindles (MS) and on tendon force from Golgi tendon organs (GTO). Most studies on low-back stabilization have focused either on intrinsic stiffness and damping (e.g., Gardner-Morse and Stokes, 2001; Brown and McGill, 2009) or on reflexes (e.g., Radebold et al., 2001) by experimentally excluding the other component or analytically merging both. This could lead to incorrect estimates, especially because changes in co-contraction could result in changes in proprioceptive reflexes and vice versa (Matthews, 1986; Kirsch et al., 1993). Therefore, combined identification is essential, but only a few studies have pursued this for low-back stabilization.

Moorhouse and Granata (2007) and Hendershot et al. (2011) identified MS feedback and intrinsic stiffness of the trunk. However, low-back stabilization was not described, since their position-driven, upper-body perturbations stabilized the trunk. Goodworth & Peterka identified low-back stabilization focussing mainly on visual (Goodworth and Peterka, 2009) and vestibular (Goodworth and Peterka, 2010) feedback, while a simplified representation of proprioceptive reflexes (only stretch velocity MS feedback) and intrinsic contributions (only stiffness) was used. Thus, a detailed analysis of the contribution of proprioceptive reflexes to low-back stabilization is still lacking.

* Corresponding author. Tel.: +31 15 278 5625; fax: +31 15 278 4717.
E-mail address: P.vanDrunen@TUDelft.nl (P. van Drunen).

0021-9290/$ - see front matter © 2013 Elsevier Ltd. All rights reserved.
http://dx.doi.org/10.1016/j.jbiomech.2013.03.007

The goal of this study was to simultaneously identify intrinsic and reflexive contributions to low-back stabilization in healthy subjects. This approach could help identify motor control deficits in LBP.

2. Methods

2.1. Subjects

Fifteen healthy adults (age, 23–58 year; mean age, 35 year) participated in this study and gave informed consent according to the guidelines of the ethical committee of VU University Amsterdam. Subjects did not experience LBP in the year prior to the experiments.

2.2. Experiments

During the experiments, subjects assumed a kneeling-seated posture, while being restrained at the pelvis (Fig. 1). A force perturbation $F_{pert}(t)$ was applied in ventral direction at the T10-level of the spine by a magnetically driven linear actuator (Servotube STB2510S Forcer and Thrustrod TRB25-1380, Copley Controls, USA). For comfort and better force transfer, a thermoplastic patch (4×4 cm) was placed between the actuator and the back of the subject. To reduce the effects of head and arm movement during the measurements, the subjects were instructed to place their hands on their head.

Visual feedback depicting the trunk rotation in sagittal (flexion/extension) and coronal (lateral bending) plane was provided to the subjects. Task instructions were to minimize the flexion/extension excursions (*Resist task*), or to relax as much as possible while limiting flexion/extension to about 15 degrees (*Relax task*). In addition, subjects were instructed in both tasks to minimize lateral flexion. Both tasks were repeated four times with the same perturbation signal.

The perturbation $F_{pert}(t)$ (Fig. 2) consisted of a dynamic disturbance of ±35 N combined with a 60 N baseline preload to maintain contact with the subject, because the actuator was not connected to the subject and therefore only capable of pushing. The dynamic disturbance (Fig. 2) was a crested multisine signal (Pintelon and Schoukens, 2001) of 20 sec duration with 18 paired frequencies, which were logarithmically distributed within a bandwidth of 0.2–15 Hz. To reduce adaptive behavior to high frequent perturbation content, the power above 4 Hz was reduced to 40% (Mugge et al., 2007). Because the perturbation was random-appearing, subjects were not expected to react with voluntary activation on the perturbation.

Each run consisted of a ramp force increase to preload level (3 s), a stationary preload (2 s), a start-up period to reduce transient behavior (the last 5 s of the dynamic disturbance), and twice the dynamic disturbance (2×20 s), which resulted in 50 s per run.

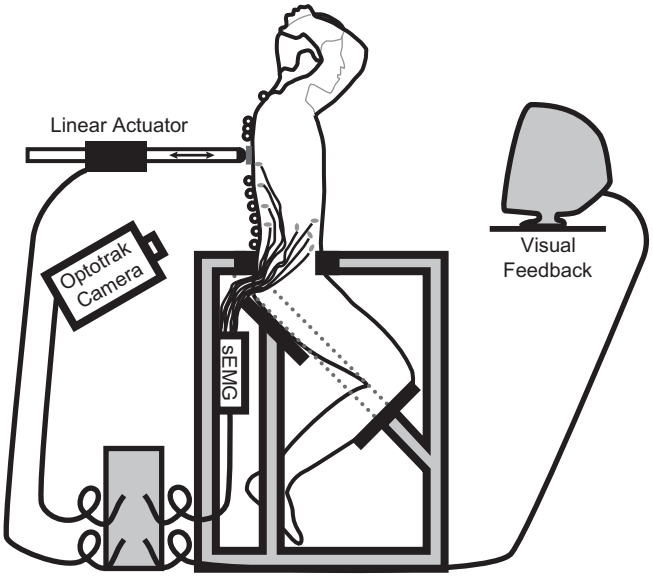

Fig. 1. Experimental setup. Subjects were restrained at the pelvis and positioned in a kneeling-seated posture, while Optotrak markers (○) and EMG electrodes are attached.

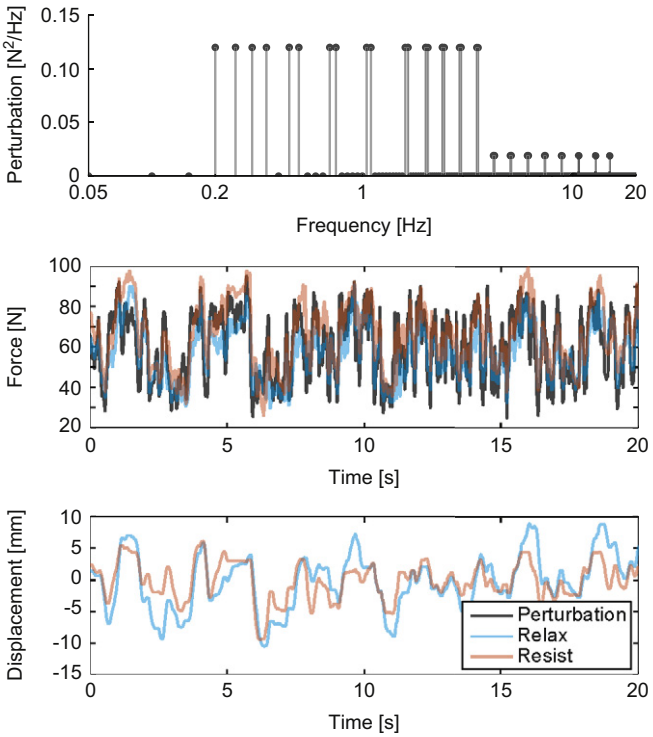

Fig. 2. The force perturbation F_{pert} (black) is projected in frequency domain (TOP) and time domain (MIDDLE). The resulting contact forces $F_c(t)$ (MIDDLE) and actuator displacements $x_A(t)$ (BOTTOM) are shown in time domain during a relax task (blue) and a resist task (red). (For interpretation of the references to color in this figure legend, the reader is referred to the web version of this article.)

2.3. Data recording and processing

Kinematics of the lumbar vertebrae (L1–L5), the thorax (T1, a cluster of markers at T6, T12), and the pelvic restraint were measured using 3D motion tracking at 100 Hz (Optotrak3020, Northern Digital Inc, Canada). The trunk rotation angle (based on markers at T12 and the pelvic restraint) in sagittal and coronal plane was provided as visual feedback to the subjects in real-time. The actuator displacement $x_A(t)$ and contact force $F_c(t)$ between the rod and the subject were measured at 2000 Hz (Servotube position sensor & Force sensor FS6-500, AMTI, USA). Trunk kinematics were described in terms of translation, since kinematic analysis indicated that an effective low-back bending rotation point, necessary to define rotations, was not well defined and inconsistent over subjects and tasks. Activity of sixteen muscles (8 bilateral pairs as listed in Table 1) was measured at 1000 Hz (surface electromyography (sEMG) Porti 17, TMSi, the Netherlands) as described in Willigenburg et al. (2010). The EMG data $e_j(t)$ (with j=#muscle) was digitally filtered (zero-phase, first-order, high-pass) at 250 Hz (Staudenmann et al., 2007) and then rectified.

All fifteen subjects showed a comparable admittance with an actuator displacement *rms* of 2.72±0.49 mm (relax) and 1.78±0.36 mm (resist). Further analysis of local low-back bending patterns (van Drunen et al., 2012) showed substantial low-back bending in eight subjects where at least 32% of the trunk rotations were attributed to bending above L5 (while measurements were not below L5) during both task instructions. In the other seven subjects, at least one task instruction resulted in less than 6% trunk rotation attributed to bending above L5, suggesting that bending below L5 and/or pelvic rotations accounted for much of the observed trunk rotations. Hence, the data collected on these subjects was not suitable for studying lumbar stabilization. Therefore, this paper will consider only the eight subjects demonstrating substantial low-back bending.

2.4. System identification

Closed loop system identification techniques (van der Helm et al., 2002; Schouten et al., 2008a) were used to estimate the translational low-back admittance ($\hat{H}_{adm}(f)$) and reflexes ($\hat{H}_{emg}(f)$) as frequency response functions (FRFs). The admittance describes the actuator displacement ($x_A(t)$) as a function of the contact force ($F_c(t)$), representing the inverse of low-back mechanical impedance. The reflexes describe the EMG data ($e_j(t)$) as a function of the actuator displacement ($x_A(t)$). Because the subjects interacted with the actuator, FRFs were estimated

Table 1
EMG Coherence ($\hat{\gamma}^2_{emg_j}(f)$) within the range of 0.2–3.5 Hz for all muscles averaged over all subjects (mean(±std)).

Muscles	Coherence	
	Relax	***Resist***
Abdominal		
Rectus abdominus	0.06 (0.05)	0.17 (0.18)
Obliquus internus	0.07 (0.07)	0.14 (0.11)
Obliquus externus (lateral)	0.10 (0.10)	0.14 (0.10)
Obliquus externus (anterior)	0.10 (0.08)	0.15 (0.10)
Back		
Longissimus (thoracic)	0.42 (0.13)	0.44 (0.13)
Iliocostalis (thoracic)	0.38 (0.14)	0.35 (0.12)
Iliocostalis (lumbar)	0.42 (0.14)	0.47 (0.10)
Longissimus (lumbar)	0.57 (0.11)	0.68 (0.08)

using closed loop methods:

$$\hat{H}_{adm}(f)=\frac{\hat{S}_{F_{pert}x_A}(f)}{\hat{S}_{F_{pert}F_c}(f)};\quad \hat{H}_{emg_j}(f)=\frac{\hat{S}_{F_{pert}e_j}(f)}{\hat{S}_{F_{pert}x_A}(f)} \tag{1}$$

with $\hat{S}_{F_{pert}x_A}(f)$ representing the estimated cross-spectral density between signals F_{pert} and x_A, etc.. The cross-spectral densities were only evaluated at the frequencies containing power in the perturbation signal. For improved estimates and noise reduction, the cross-spectral densities were averaged across the 8 time segments per task (four repetitions each containing two 20 s segments) and over 2 adjacent frequency points (Jenkins & Watts, 1969). Finally, $\hat{S}_{F_{pert}e_j}(f)$ was averaged over the left and right muscles.

The coherence associated with $\hat{H}_{adm}(f)$ and $\hat{H}_{emg}(f)$ was derived as:

$$\hat{\gamma}^2_{adm}(f)=\frac{|\hat{S}_{F_{pert}x_A}(f)|^2}{\hat{S}_{F_{pert}F_{pert}}(f)\hat{S}_{x_Ax_A}(f)};\quad \hat{\gamma}^2_{emg_j}(f)=\frac{|\hat{S}_{F_{pert}e_j}(f)|^2}{\hat{S}_{F_{pert}F_{pert}}(f)\hat{S}_{e_je_j}(f)} \tag{2}$$

Coherence ranges from zero to one, where one reflects a perfect, noise-free relation between input and output. Since spectral densities were averaged over 16 points, a coherence greater than 0.18 is significant with $P<0.05$ (Halliday et al., 1995).

2.5. Parametric identification

A linear neuromuscular control (NMC) model was constructed to translate the FRFs into physiological elements representing intrinsic and reflexive contributions (Fig. 3). The intrinsic contribution consists of the trunk mass (m), and the lumbar stiffness and damping (k, b). The reflexive contribution involves the lumbar muscle spindle (MS) position and velocity feedback gains (k_P, k_V) and the Golgi tendon organ (GTO) force feedback gain (k_F), both with a time delay (τ_{REF}). Muscle activation dynamics were implemented as a second order system (Bobet and Norman, 1990) with a cut-off frequency (f_{ACT}) and a dimensionless damping (d_{ACT}). Contact dynamics between the subjects' trunk and the actuator were included as a damper and a spring (b_C, k_C). The activation signal ($A(t)$) in the model was scaled to the EMG data using a scaling parameter (e_{SCALE}). Several other model configurations were explored by removing some elements and/or including vestibular acceleration feedback (k_{VEST}, τ_{VEST}), MS acceleration feedback (k_A), separate time delays for the MS (τ_{MS}) and the GTO (τ_{GTO}) feedback pathways, or a second DOF representing a head mass connected to the torso by a spring and damper (m_H, b_H, k_H).

The parameters were identified by fitting the NMC-model on the FRFs of both the low-back admittance and the reflexive muscle activation for all repetitions. The relax and resist task were optimized simultaneously assuming masses, time delays, activation and contact dynamics, and EMG-scaling to be constant over conditions. The criterion function used in the estimation was:

$$err=\sum_{1}^{\#rep}\sum_{k}\frac{\hat{\gamma}^2_{adm}(f_k)^2}{1+f_k}\left|\log\left(\frac{\hat{H}_{adm}(f_k)}{H^{mdl}_{adm}(f_k)}\right)\right|^2 + q\sum_{1}^{\#rep}\sum_{k}\frac{\hat{\gamma}^2_{emg}(f_k)^2}{1+f_k}\left|\log\left(\frac{\hat{H}_{emg}(f_k)}{H^{mdl}_{emg}(f_k)}\right)\right|^2 \tag{3}$$

with f_k as the power containing frequencies, and $H^{mdl}_{adm}(f_k)$ and $H^{mdl}_{emg}(f_k)$ as the transfer functions of the model. The criterion describes the goodness of fit of the complex admittance (upper term) and reflexive muscle activity (lower) term where the weighting factor q was selected to be 0.25 to provide equal contribution of the admittance and reflexive muscle activity to the criterion function.

2.6. Model validation

The accuracy of the parameters was evaluated using the Standard Error of the Mean (*SEM*) (Ljung, 1999):

$$SEM=\frac{1}{N}diag\left[(J_p^TJ_p)^{-1}\right]\sum err^2 \tag{4}$$

where the Jacobian J_p contains the gradient to the optimal parameter vector p of the predicted error *err*. The more influence a parameter has on the optimization criterion, the smaller the *SEM* will be.

The validity of the optimized model and its parameters was assessed in the time domain using the variance accounted for (*VAF*). A *VAF* of 100% reflects a perfect description of the measured signal by the model. The experimental measurements $x_A(t)$ were compared with the estimated model outcomes $\hat{x}_A(t)$:

$$VAF_x=\left[1-\frac{\Sigma_1^n(x_A(t_n)-\hat{x}_A(t_n))^2}{\Sigma_1^n(x_A(t_n))^2}\right]\times 100\% \tag{5}$$

where n is the number of data points in the time signal. For the EMG, VAF_e was calculated by replacing $x_A(t)$ and $\hat{x}_A(t)$ with $e_j(t)$ and $\hat{e}_j(t)$, respectively. To reduce noise contributions, measured data was reconstructed with only the frequencies that contain power in the perturbation.

2.7. Statistics

Significance ($P<0.05$) in effects of task instruction on the FRF gains and the model parameters was evaluated with a repeated-measures ANOVA. For the FRF gains only the first five frequency points (e.g., a bandwidth of 0.2–1.1 Hz) were analyzed, because effects of task instruction were negligible at higher frequencies.

3. Results

3.1. Frequency response functions (FRFs)

Human low-back stabilizing behavior is described by the FRFs of the admittance and the reflexes (Fig. 4), while high coherences indicate good input–output correlation. The coherence of the admittance was above 0.8 for the resist task, and above 0.75 for the relax task up to 3.5 Hz ($\hat{\gamma}^2_{adm}>0.55$ over the whole frequency range). As shown in Table 1, the coherence levels of the abdominal muscles were generally insignificant ($\hat{\gamma}^2_{emg}<0.18$), resulting in the

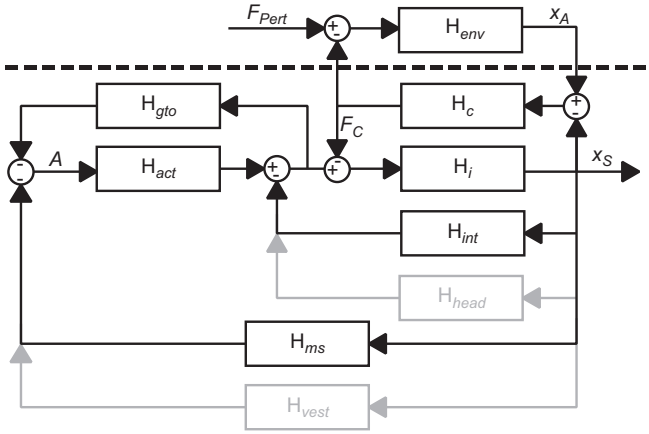

Fig. 3. The model structure. The signals force perturbation ($F_{pert}(t)$), contact force ($F_c(t)$), actuator displacements ($x_A(t)$), the spinal discplacement ($x_S(t)$), and muscle activity ($A(t)$) are displayed. Involved are the dynamics of the trunk inertia ($H_I=1/(ms^2)$) and intrinsic properties ($H_{INT}=bs+k$), the head ($H_{HEAD}=m_Hs^2(b_Hs+k_H)/(m_Hs^2+b_Hs+k_H)$), the contact point ($H_C=b_Cs+k_C$), the actuator environment ($H_{ENV}=1/(m_{ENV}\ s^2+b_{ENV}\ s+k_{ENV})$), and the muscle activation dynamics ($H_{ACT}=(2\pi f_{ACT})^2/(s^2+4\pi f_{ACT}d_{ACT}\ s+(2\pi f_{ACT})^2)$). Reflexive feedback is described by muscle spindles ($H_{MS}=(k_As^2+k_Vs+k_P)e^{-\tau_{ref}s}$)) of which the acceleration component k_A is optional, Golgi tendon organs ($H_{GTO}=k_F\ e^{-\tau_{ref}s}$) and the vestibular organs ($H_{VEST}=k_{VEST}\ e^{-\tau_{VEST}s}$). The gray pathways are only implemented during the explorative model search, as well as the division of τ_{REF} into time delays for the MS (τ_{MS}) and GTO (τ_{GTO}).

exclusion of the abdominal muscles from further analysis. Between 0.2 and 3.5 Hz, significant coherences were found for all dorsal muscles (Table 1), of which the lumbar part of the Longissimus muscle was the highest with an average coherence of 0.57. This is considered high given the noisy character of sEMG measurements and the number of muscles involved in trunk stabilization. Therefore, the lumbar part of the Longissimus muscle was used for modeling.

The low-back admittance FRF resembles a second order system (i.e., a mass-spring-damper system). The high-frequency behavior (>4 Hz) is mainly influenced by trunk mass combined with contact dynamics. The low-frequency response (<1 Hz) reflects intrinsic stiffness and reflexive behavior. The intermediate frequencies are dominated by the intrinsic damping and reflexive responses. The reflexive FRF reflects position feedback (low-frequency flat gain), velocity feedback (intermediate frequencies) and force and/or acceleration feedback (high-frequency second-order ramp-up).

3.2. Identification of intrinsic and reflexive parameters

To select the most appropriate model structure, eight explorative model configurations were compared by evaluating their *VAF* and *SEM* values (Table 2). All model configurations included the trunk mass, lumbar stiffness and damping, and contact dynamics. This intrinsic model (1) described the displacements well (VAF_x=87%), but could not describe the EMG due to the lack of reflexes. Adding MS feedback to the intrinsic model (2) slightly improved the displacement *VAF* (90%), but described the EMG measurements only reasonably well (VAF_e=28%). To describe the second order reflexive characteristics, a MS acceleration component (3) associated with MS nonlinearity (Schouten et al., 2008a) or a vestibular acceleration component (4) were included. These resulted in a comparable VAF_x and a better description of the EMG (VAF_e=35% and 32%). The second order reflexive characteristics can also indicate force feedback from the GTO. A model including MS and GTO feedback (5) resulted in slightly higher VAF_e (39%) and

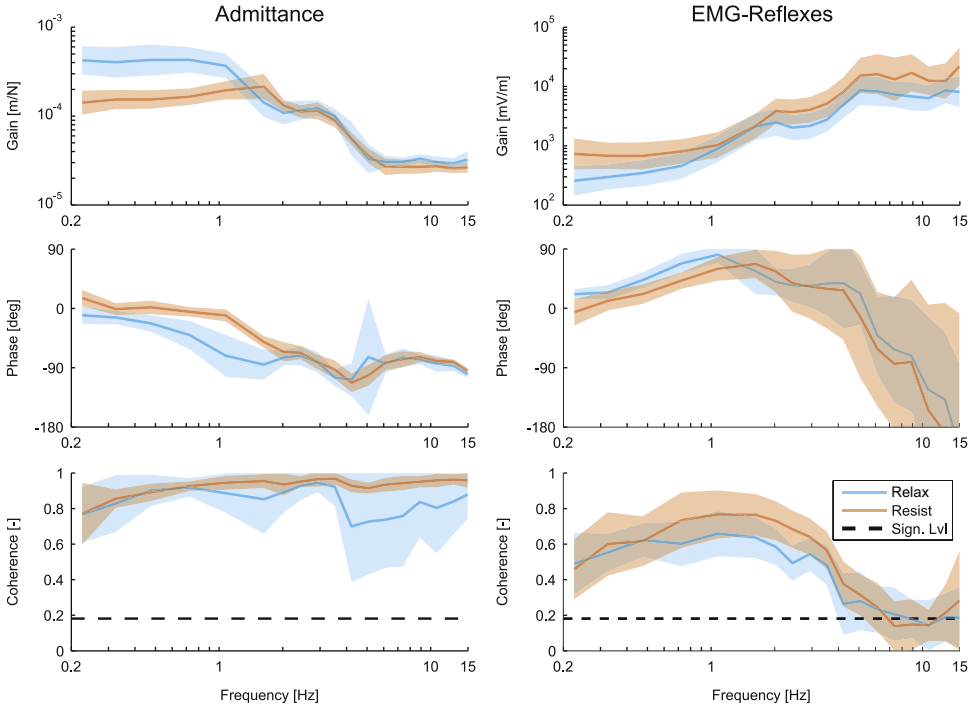

Fig. 4. The FRFs and coherences of the human low-back admittance (left) and EMG reflexes of the Longissimus Muscle (right) averaged over all subjects for the relax task (blue) and resist task (red). Shadings represent the standard deviations. (For interpretation of the references to color in this figure legend, the reader is referred to the web version of this article.)

Table 2
Results of different model configurations: The variance accounted for (VAF) and percentage Standard Errors of the Mean of parameter values (%SEM) averaged over all subjects and parameters (mean(±std)). The intrinsic model includes trunk inertia, intrinsic properties and contact dynamics. Feedback from the muscle spindles (MS), the vestibular organ (Vest) and Golgi tendon organ (GTO) has been added as well as a head mass (Head), an acceleration component from the muscle spindles (MS_{acc}), and separate time delays for the MS and GTO (τ_{MS} & τ_{GTO}).

Model options	VAF_x [%]		VAF_e [%]		%SEM
	Relax	*Resist*	*Relax*	*Resist*	
(1) Intrinsic	88.3 (07.6)	85.7 (7.0)	–	–	12
(2) Intrinsic+MS	89.3 (07.3)	90.0 (4.1)	25.1 (26.4)	30.5 (31.0)	22
(3) Intrinsic+MS+MS_{acc}	89.3 (07.5)	90.7 (3.6)	26.8 (26.6)	43.9 (09.8)	21
(4) Intrinsic+MS+Vest	89.3 (07.5)	90.7 (3.5)	31.7 (17.5)	33.2 (24.1)	337
(5) Intrinsic+MS+GTO	89.4 (07.4)	89.9 (4.5)	37.2 (19.1)	40.8 (20.9)	38
(6) Intrinsic+MS+GTO (τ_{MS} & τ_{GTO})	89.1 (07.2)	89.7 (3.8)	31.9 (29.0)	42.7 (18.1)	77
(7) Intrinsic+MS+GTO+Vest	39.9 (16.1)	45.8 (6.4)	64.2 (07.1)	35.8 (07.1)	502e3
(8) Intrinsic+MS+GTO+Head	89.3 (07.3)	90.7 (3.4)	36.7 (26.1)	44.3 (20.9)	165

comparable VAF_x (90%). Including more components and parameters in the model by assigning separate time delays for the MS and GTO (6), combining the MS, GTO and vestibular feedback (7) or adding an extra DoF representing the head mass (8) resulted in comparable VAFs; however, poor *SEM* values indicated over-parameterization resulting in decreased reliability of the estimated parameters for these models. For further analysis the intrinsic model with MS and GTO feedback (5) was selected, as it contained the essential intrinsic and reflexive components for which *SEM* values (average 38% of parameter values) indicated a reliable estimate of the parameters.

Figs. 5 and 6 illustrate the fit of the model predictions to the measured FRFs and time history data, respectively. An accurate fit was obtained up to around 3.5 Hz, with some deviations at higher frequencies which are also apparent in the EMG time history data. After removing the high frequent deviations in the EMG by a 3.5 Hz low-pass filter, a VAF_e of 55% was obtained, indicating a good fit at frequencies with high coherence values. Considering the variation in gender and age of the subject group, parameter estimates (Fig. 7) were consistent over subjects. Only the estimated MS velocity feedback gain k_V was inconsistent over subjects and seems of minor importance as evidenced by high SEM values, and the fact that model (5) described the data almost as well when k_V was excluded.

3.3. Task

Subjects modulated low-back stabilization with task instruction, where admittance below 1.1 Hz in the resist task was 61% lower ($P<0.02$) than in the relax task. At frequencies above 2 Hz, admittance was not affected by task instructions. The reflex FRF-gain was task dependent below 1.1 Hz and increased by 73% ($P<0.03$) for the resist task. Underlying these differences, the resist task coincided with significantly higher intrinsic stiffness ($P<0.003$), position feedback ($P<0.0002$) and force feedback ($P<0.05$), while intrinsic damping and velocity feedback were not significantly different between tasks.

3.4. Intrinsic and reflexive contributions

The reflexive contribution to low-back stabilization is illustrated simulating the admittance of the complete model (5) and removing GTO and/or MS feedback (Fig. 8). Note that parameters of the simplified models were not re-estimated and do not represent the best possible fit. Differences were primarily observed at the lower frequencies. Surprisingly, the model without reflexive feedback yielded a slightly lower admittance than the complete model. As expected MS reflexes reduced the admittance and the GTO reflexes increased the admittance. Against our expectations, the effect of the GTO was stronger than the effect of MS, resulting in a small net increase in admittance due to feedback. This net increase in admittance due to reflex feedback was consistent over all models including reflexes (2–8), but the reflexive pathway to which the effect was attributed varied.

4. Discussion

The goal of this study was to simultaneously identify intrinsic and reflexive contributions to low-back stabilization in healthy subjects.

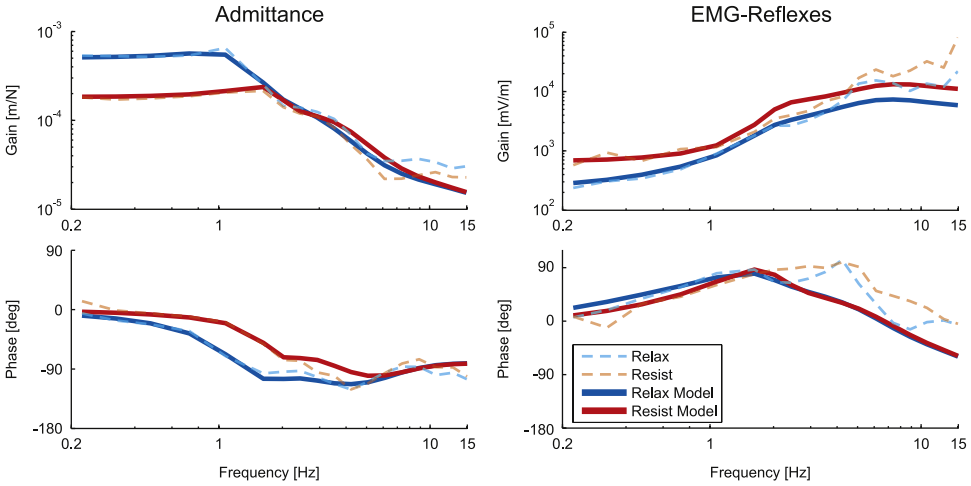

Fig. 5. Model predictions (dark, solid) versus the measured data (light, dashed) of the admittance (left) and the EMG reflexes of Longissimus muscle (right) for one typical subject during a relax task (blue) and a resist task (red). (For interpretation of the references to color in this figure legend, the reader is referred to the web version of this article.)

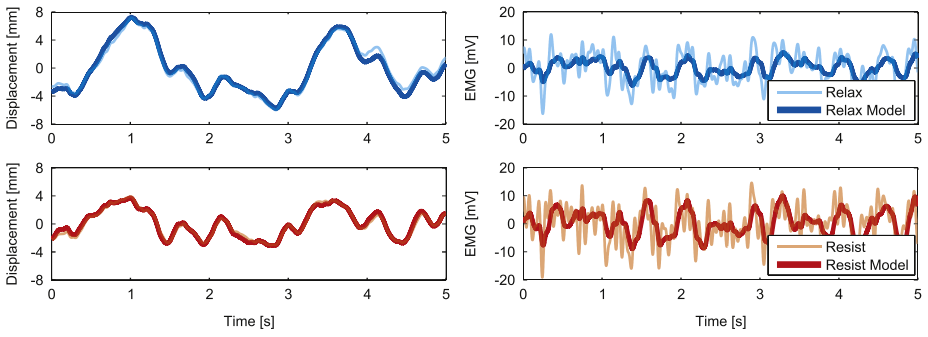

Fig. 6. Model predictions (dark) versus the measured data (light) of the displacement (left) and the EMG of Longissimus muscle (right) for one typical subject during a relax task (blue) and a resist task (red). (For interpretation of the references to color in this figure legend, the reader is referred to the web version of this article.)

Upper-body sway was evoked using continuous force perturbations at the trunk, while subjects performed a resist or relax task. Frequency Response Functions (FRFs) and coherences of the admittance (kinematics) and reflexes (EMG) were obtained. Finally, intrinsic and proprioceptive parameters were captured by a physiological model. This methodology allowed for quantification of the intrinsic and proprioceptive feedback contributions simultaneously.

The FRFs of admittance and reflexes showed a consistent response in all subjects. High coherences were found for the admittance (across tested bandwidth) and the reflexes (upto 3.5 Hz). In comparison with the relax task, the resist task resulted in a 61% decrease in admittance and a 73% increase in reflex gain below 1.1 Hz. In only eight subjects substantial low-back bending was found, resulting in exclusion of the other seven subjects and a limited sample size for statistics.

Several model configurations were explored. All configurations were based on physiological elements with the intrinsic system (trunk mass, and lumbar stiffness and damping) as core structure, which predicted the kinematics effectively. Therefore, sEMG measurements were included to identify the reflexive components. A model configuration including the intrinsic system and MS (position and velocity) and GTO (force) feedback described an average of 90% of the variance in low-back displacements and 39% of the variance in EMG measurements (VAF_e of 55% up to 3.5 Hz). This is reasonable, given that the low-back contains five vertebrae and multiple muscles and was described by a 1-DoF model with only one lumped flexor/extensor muscle where feedback parameters were estimated using the Longissimus muscle disregarding reflexes of deeper muscles. Although vestibular and visual feedback are expected to contribute to low-back stabilization (Goodworth and Peterka, 2009), our measurements do not contain enough information to separately include their contributions (poor reliability of the estimated parameters). Including extra vestibular (e.g., galvanic vestibular stimulation) and/or visual stimuli could give more information about these feedback systems.

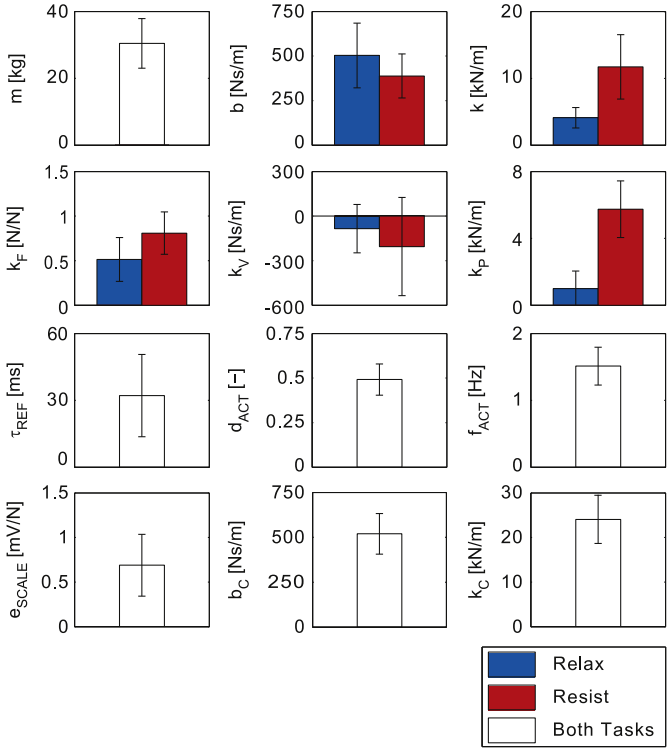

Fig. 7. Subject-averaged estimated parameters. The error bars represent the standard deviations. The parameters modulated due to task instruction have different estimated values for the relax task (red) and the resist task (blue). (For interpretation of the references to color in this figure legend, the reader is referred to the web version of this article.)

The estimated trunk mass (30.4 kg) was comparable with values in Moorhouse and Granata (2005), while the estimated intrinsic damping (503.3 Ns/m) and stiffness (4.1 kN/m) during the relax task were higher, because (inhibitory) GTO reflexes were not included in their study, and possibly because the hand-position on the head in the current experimental setup results in higher stabilization demands. The estimated reflex time delay of 32.1 ms is within the expected (short-latency) range (Goodworth and Peterka, 2009). For the resist task, increased intrinsic stiffness (from 4.1 to 11.7 kN/m) was found similar to Gardner-Morse and Stokes (2001) and Granata and Rogers (2007), where increased muscle activation led to increased intrinsic stiffness. Also the proprioceptive feedback gains modulated with task instruction. Position-referenced information seems to be more important for a resist task, because the model showed a strong increase in MS position feedback. The resist task led to an increased GTO force feedback, but was not consistent over all subjects. A separate analysis with the NMCLab Graphical User Interface (Schouten et al., 2008b) showed that a GTO force feedback gain increase had a stabilizing effect on the system, which allows for an increase of the 'destabilizing' MS pathways. On the other hand, a decrease of the GTO force feedback gain led to less inhibitory effects of the intrinsic and MS pathways and thus to more resistance.

The model variations in Fig. 8, indicate that reflexes reduce the overall resistance in both the resist and the relax task. The model attributes a substantial resistance to the intrinsic stiffness and damping, a minor resistance to MS feedback, while GTO feedback strongly reduces the resistance. Such an effect of force feedback has been previously reported in relax tasks as well as in tasks where the force levels need to be controlled (Mugge et al., 2010). However, we are not aware of studies showing a reduced resistance due to GTO force feedback for resist tasks or position control, especially not where this leads to a net resistance reduction by all reflexes combined.

Finally, this study proposed a method to identify intrinsic and reflexive contributions to low-back stabilization and applied this

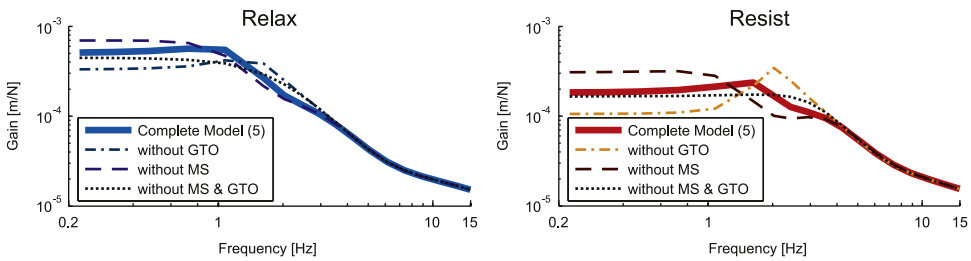

Fig. 8. Effect of MS and GTO feedback illustrated using NMC models of a typical subject during a relax (blue) and resist (red) task. The admittance of the complete model including MS and GTO feedback is given as reference (solid). The other lines represent this model without GTO feedback (dashed) and without GTO and MS feedback (dotted). (For interpretation of the references to color in this figure legend, the reader is referred to the web version of this article.)

method on a group of healthy subjects. Future studies should apply this method to LBP patients, to determine whether motor control deficits can be identified.

Conflicts of interest statement

The authors declare that no conflict of interest were associated with the present study.

Acknowledgments

This research is supported by the Dutch Technology Foundation STW, which is part of the Netherlands Organisation for Scientific Research (NWO) and partly funded by the Ministry of Economic Affairs, Agriculture and Innovation. See www.neurosipe.nl—Project 10732: QDISC.

The authors would like to express the sincere gratitude to Jos D. van den Berg for the realization of the experimental setup and to Nienke W. Willigenburg, MSc, for her contributions in preparing and performing the measurements.

References

Bergmark, A., 1989. Stability of the lumbar spine—a study in mechanical engineering. Acta Orthopaedica Scandinavica 60, 3–54.

Bobet, J., Norman, R.W., 1990. Least-squares identification of the dynamic relation between the electromyogram and joint moment. Journal of Biomechanics 23, 1275–1276.

Brown, S.H.M., McGill, S.M., 2009. The intrinsic stiffness of the in vivo lumbar spine in response to quick releases: implications for reflexive requirements. Journal of Electromyography and Kinesiology 19, 727–736.

Cholewicki, J., Polzhofer, G.K., Radebold, A., 2000. Postural control of trunk during unstable sitting. Journal of Biomechanics 33, 1733–1737.

Crisco, J.J.I., Panjabi, M.M., 1991. The intersegmental and multisegmental muscles of the lumbar spine: a biomechanical model comparing lateral stabilizing potential. Spine 16, 793–799.

Gardner-Morse, M.G., Stokes, I.A.F., 2001. Trunk stiffness increases with steady-state effort. Journal of Biomechanics 34, 457–463.

Goodworth, A.D., Peterka, R.J., 2009. Contribution of sensorimotor integration to spinal stabilization in humans. Journal of Neurophysiology 102, 496–512.

Goodworth, A.D., Peterka, R.J., 2010. Influence of bilateral vestibular loss on spinal stabilization in humans. Journal of Neurophysiology 103, 1978–1987.

Granata, K.P., Rogers, E., 2007. Torso flexion modulates stiffness and reflex response. Journal of Electromyography and Kinesiology 17, 384–392.

Halliday, D.M., Rosenberg, J.R., Amjad, A.M., Breeze, P., Conway, B.A., Farmer, S.F., 1995. A framework for the analysis of mixed time series/point process data—theory and application to the study of physiological tremor, single motor unit discharges and electromyograms. Progress in Biophysics and Molecular Biology 64, 237–278.

Hendershot, B., Bazrgari, B., Muslim, K., Toosizadeh, N., Nussbaum, M.A., Madigan, M.L., 2011. Disturbance and recovery of trunk stiffness and reflexive muscle responses following prolonged trunk flexion: influences of flexion angle and duration. Clinical Biomechanics 26, 250–256.

Jenkins, G.M., Watts, D.G., 1969. Spectral analysis and its applications. Holden-Day, San Francisco, USA.

Kirsch, R.F., Kearney, R.E., MacNeil, J.B., 1993. Identification of time-varying dynamics of the human triceps surae stretch reflex. Experimental Brain Research 97, 115–127.

Ljung, L., 1999. System Identification: Theory for the User, 2nd Edition PTR Prentice Hall, Upper Saddle River, USA.

Loney, P.L., Stratford, P.W., 1999. The prevalence of low back pain in adults: a methodological review of the literature. Physical Therapy 79, 384–396.

Matthews, P.B.C., 1986. Observations of the automatic compensation of reflex gain on varying the pre-existing level of motor discharge in man. Journal of Physiology 374, 73–90.

Moorhouse, K.M., Granata, K.P., 2007. Role of reflex dynamics in spinal stability: intrinsic muscle stiffness alone is insufficient for stability. Journal of Biomechanics 40, 1058–1065.

Moorhouse, K.M., Granata, K.P., 2005. Trunk stiffness and dynamics during active extension exertions. Journal of Biomechanics 38, 2000–2007.

Mugge, W., Abbink, D., Schouten, A., Dewald, J., van der Helm, F., 2010. A rigorous model of reflex function indicates that position and force feedback are flexibly tuned to position and force tasks. Experimental Brain Research 200, 325–340.

Mugge, W., Abbink, D.A., van der Helm, F.C.T., 2007. Reduced power method: how to evoke low-bandwidth behavior while estimating full-bandwidth dynamics. In: Proceedings of the IEEE 10th International Conference on Rehabilitation Robotics (ICORR), Noordwijk aan Zee (The Netherlands).

Picavet, H.S.J., Schouten, J.S.A.G., 2003. Musculoskeletal pain in the Netherlands: prevalences, consequences and risk groups, the DMC3-study. Pain 102, 167–178.

Pintelon, R., Schoukens, J., 2001. System Identification: A Frequency Domain Approach. John Wiley & Sons, New York, USA.

Radebold, A., Cholewicki, J., Polzhofer, G.K., Greene, H.S., 2001. Impaired postural control of the lumbar spine is associated with delayed muscle response times in patients with chronic idiopathic low back pain. Spine 26, 724–730.

Schouten, A.C., de Vlugt, E., van Hilten, J.J.B., van der Helm, F.C.T., 2008a. Quantifying proprioceptive reflexes during position control of the human arm. IEEE Transactions on Biomedical Engineering 55, 311–321.

Schouten, A.C., Mugge, W., van der Helm, F.C.T., 2008b. NMClab, a model to assess the contributions of muscle visco-elasticity and afferent feedback to joint dynamics. Journal of Biomechanics 41, 1659–1667.

Staudenmann, D., Potvin, J.R., Kingma, I., Stegeman, D.F., van Dieën, J.H., 2007. Effects of EMG processing on biomechanical models of muscle joint systems: Sensitivity of trunk muscle moments, spinal forces, and stability. Journal of Biomechanics 40, 900–909.

van den Hoogen, H.J.M., Koes, B.W., van Eijk, J.T.M., Bouter, L.M., Devillé, W., 1998. On the course of low back pain in general practice: a one year follow up study. Annals of the Rheumatic Diseases 57, 13–19.

van der Helm, F.C.T., Schouten, A.C., de Vlugt, E., Brouwn, G.G., 2002. Identification of intrinsic and reflexive components of human arm dynamics during postural control. Journal of Neuroscience Methods 119, 1–14.

van Dieën, J.H., Selen, L.P.J., Cholewicki, J., 2003. Trunk muscle activation in low-back pain patients, an analysis of the literature. Journal of Electromyography and Kinesiology 13, 333–351.

van Drunen, P., Maaswinkel, E., Veeger, H.E.J., van Dieën, J.H., Happee, R., 2012. Spinal bending patterns in sagittal plane perturbations. In: Proceedings of the 19th Congress of the International Society of Electrophysiology and Kinesiology (ISEK), Brisbane (Australia).

Willigenburg, N., Kingma, I., van Dieën, J., 2010. How is precision regulated in maintaining trunk posture? Experimental Brain Research 203, 39–49.